American Journal of Pathology, Vol. 168, No. 6, June 2006

DOI: 10.2353/ajpath.2006.050588

Vascular Biology, Atherosclerosis and Endothelium Biology

Inhibition of Platelet-Derived Growth Factor B Signaling Enhances the Efficacy of Anti-Vascular Endothelial Growth Factor Therapy in Multiple Models of Ocular Neovascularization

Nobuo Jo, Carolina Mailhos, Meihua Ju, Eunice Cheung, John Bradley, Kazuaki Nishijima, Gregory S. Robinson, Anthony P. Adamis, and David T. Shima

Eyetech Research Center, Lexington, Massachusetts

'Vascular endothelial growth factor-A (VEGF-A) blockade has been recently validated as an effective strategy for the inhibition of new blood vessel growth in cancer and ocular pathologies. However, several studies have also shown that anti-VEGF therapy may not be as effective in the treatment of established unwanted blood vessels, suggesting they may become less dependent on VEGF-A for survival. The VEGF-A dependence of vessels may be related to the presence of vascular mural cells (pericytes or smooth muscle cells). Mural cell recruitment to the growing endothelial tube is regulated by platelet-derived growth factor-B (PDGF-B) signaling, and interference with this pathway causes disruption of endothelial cell-mural cell interactions and loss of mural cells. We have investigated the basis of blood vessel dependence on VEGF-A in models of corneal and choroidal neovascularization using a combination of reagents (an anti-VEGF aptamer and an anti-PDGFR-β antibody) to inhibit both the VEGF-A and PDGF-B signaling pathways. We demonstrate that neovessels become refractory to VEGF-A deprivation over time. We also show that inhibition of both VEGF-A and PDGF-B signaling is more effective than blocking VEGF-A alone at causing vessel regression in multiple models of neovascular growth. These findings provide insight into blood vessel growth factor dependency and validate a combination therapy strategy for enhancing the current treatments for ocular angiogenic disease. ***(Am J Pathol 2006, 168:2036–2053; DOI: 10.2353/ajpath.2006.050588)***

Angiogenesis is a major component in several pathological processes, including tumor growth, chronic inflammatory diseases, and ocular diseases.[1–3] In ocular diseases characterized by aberrant angiogenesis, neovascularization (NV) has catastrophic effects on vision leading to hemorrhage, edema, and ultimately blindness.[4] Although multiple stimuli may be involved in the development of ocular NV, vascular endothelial growth factor A (VEGF-A), a specific endothelial cell mitogen as well as a permeability and survival factor, plays a major role in this process.[5–7] Antagonism of the VEGF-A pathway results in inhibition of blood vessel growth in several forms of ocular NV, including NV of the iris,[7] the cornea,[8] the retina,[9] and the choroid.[10] These preclinical studies predict that antagonizing VEGF-A is a viable approach for the treatment of ocular NV. Indeed, an anti-VEGF aptamer (EYE001, the drug substance in Macugen, Eyetech Pharmaceuticals Inc., New York, NY) is now approved for the treatment of the wet form of age-related macular degeneration. However, there is also evidence that anti-VEGF therapy alone may not be sufficient to cause vessel regression in advanced stages of aberrant angiogenesis and consequently may have a more limited ability to impact established disease. Several studies have suggested that the response of blood vessels to anti-VEGF therapy is influenced by vessel maturation,[11,12] a rather ill-defined state that is commonly attributed to the presence of vascular mural cells (MCs, pericytes around capillaries and smooth muscle cells around larger vessels).

Mural cells are required for normal vascular stability and function.[13,14] The recruitment of MCs to endothelial cells (ECs) requires platelet-derived growth factor B

N.J. and C.M. contributed equally to this work.

Accepted for publication February 28, 2006.

Address reprint requests to David T. Shima, Eyetech Research Center, 35 Hartwell Ave., Lexington, MA 02421. E-mail: david.shima@eyetech.com.

(PDGF-B) and signaling through the PDGF receptor-type β (PDGFR-β). Transgenic mice lacking PDGF-B and PDGFR-β fail to recruit MCs to new blood vessels, resulting in abnormal vessel stabilization and maturation.[15–17] Furthermore, inhibition of PDGF-B signaling by an anti-PDGFR-β antibody[18] causes disruption of EC/MC association and destabilization of the developing retinal vasculature. These studies suggest that MCs are critically involved in normal vasculature formation and that MC recruitment in developmental angiogenesis depends on PDGF-B and PDGFR-β. However, little is known about the importance of MC recruitment and EC/MC interaction in pathological angiogenesis of solid tumors and ocular disease. In vitro studies have shown that VEGF-A produced by MCs may act in a juxtacrine/paracrine manner as a survival and stabilizing factor for ECs in microvessels.[19] In addition, MCs that surround tumor vessels produce VEGF-A,[20,21] and tumor vessels lacking MCs are more dependent on VEGF-A for their survival than vessels associated with MCs,[12] suggesting that MCs protect endothelial cells in situations of decreasing VEGF-A. Consequently, anti-VEGF therapy may be affected by the presence of MCs. A combination of inhibitors, targeting receptor tyrosine kinases (RTKs) in both ECs and MCs, were recently shown to inhibit the growth of mouse insulinomas better than any single RTK blocker.[22] Also, an RTK inhibitor targeting VEGFR-2 and PDGFR-β was recently shown to cause potent tumor vessel regression, a finding that was attributed to the combined interference with both VEGF-A signaling and EC/MC interaction.[23] However, interference with PDGF-B signaling has been shown to decrease interstitial pressure and increase the uptake of substances by tumors. Therefore, the increased access of VEGF-A inhibitors to the tumor microenvironment alone could explain the increased efficacy of the combination RTK approach.[24,25]

To investigate if depleting MCs would enhance the effect of an anti-VEGF blockade on neovessels and whether this blockade remained effective over time, we compared using VEGF and PDGFR-β inhibitors alone and in combination for the treatment of ocular angiogenesis. A previous study has shown that systemic administration of an anti-mouse PDGFR-β antibody completely blocked MC recruitment to blood vessels in the neonatal mouse retina.[18] We show that MC loss, following PDGF-B signaling inhibition, renders growing vessels more sensitive to the anti-VEGF blockade. In addition, we demonstrate the effect of blocking either PDGF-B or VEGF-A signaling alone or in combination in two models of pathological NV in the eye, corneal NV, and choroidal NV (CNV). There are distinct advantages to studying both models of ocular NV: CNV is the trademark of age-related macular degeneration, the leading cause of blindness among the elderly in industrialized countries.[26] Corneal NV, on the other hand, allows clear visualization of abnormal vascular growth. In addition, the vessels that grow into the normally avascular cornea following circumferential depletion of the corneal and limbal epithelium become well established and show no natural regression, making this an attractive model to study vessel regression. In this report, we directly demonstrate that the efficacy of a VEGF-A blockade diminishes as neovessels persist over time, and that specific targeting of *both* VEGF-A and PDGF-B signaling pathways is more effective at preventing and regressing pathological ocular NV than targeting VEGF-A signaling alone.

Materials and Methods

Animals and Anesthesia

C57BL/6 mice from Charles River (Wilmington, MA) were treated in accordance with the Association for Research in Vision and Ophthalmology Statement for the Use of Animals in Ophthalmic and Vision Research. Animals were anesthetized with intramuscular ketamine hydrochloride (25 mg/kg) and xylazine (10 mg/kg), and their pupils were dilated with 1% tropicamide. Mice were euthanized with an overdose of ketamine and xylazine administrated by intraperitoneal injection. Adult (6-week-old) male mice were used to generate corneal NV or CNV models. Experimental groups consisted of five animals per group unless otherwise stated.

Antibodies and Reagents

ECs were detected using an antibody against platelet-endothelial cell adhesion molecule-1 (PECAM-1, clone MEC 13.3; BD Biosciences Pharmingen, San Diego, CA). ECs were also visualized using fluorescein isothiocyanate-coupled concanavalin A lectin or biotinylated *Griffonia simplicifolia* lectin B4 obtained from Vector Laboratories (Burlingame, CA). The choice of EC detection reagent sometimes depended on whether the rat APB5 antibody was used in the experiment to avoid cross-reactivity between APB5 and PECAM-1 (also a rat monoclonal antibody). We found no difference in EC detection by all three methods. MCs were detected using an antibody against smooth muscle actin (SMA, clone 1A4; Sigma-Aldrich, St. Louis, MO), an antibody against PDGFR-β (clone APB5; eBioscience, San Diego, CA), or an antibody against NG2 (Chemicon, Temecula, CA). Cells in S phase of the cell cycle were detected using an antibody against phospho-histone H3 (Ser10; Upstate Biotechnology, Inc., Lake Placid, NY). Alexa 488- and 546-conjugated secondary antibodies were from Molecular Probes (Eugene, OR). As an anti-VEGF-A reagent, we used the active compound in Macugen, pegaptanib sodium, which is a pegylated anti-$VEGF_{165}$ aptamer (EYE001, Eyetech Pharmaceuticals). The anti-$VEGF_{165}$ aptamer is an oligonucleotide (28 ribonucleotide bases) that binds to the exon-7-encoded domain of human VEGF with high specificity and affinity.[27] It does not bind to VEGF-A isoforms lacking this domain such as $VEGF_{120(121)}$. The oligonucleotide is conjugated to a 40-kd polyethylene glycol moiety to increase its half-life and will be referred to in this report as the anti-VEGF aptamer or aptamer. The dose and the evaluation time points were based on a previous report.[28] To block PDGFR-β signaling, we used either a monoclonal antibody directed against murine PDGFR-β (clone APB5;

e-Bioscience) or Gleevec (Novartis Pharma AG, Basel, Switzerland), an inhibitor of PDGF receptors, c-kit, and BCR-ABL tyrosine kinases. Phosphate-buffered saline (PBS) was used as a control in all experiments unless otherwise stated. We verified that it behaved similarly to scrambled aptamer, polyethylene glycol alone,[29] and an isotype-matched antibody control for APB5 (data not shown).

Corneal Neovascularization Model

A previously described mouse model of corneal NV[30] was used in this study with the following modification: NaOH (2 μl of 0.2 mmol/L) was applied topically to the eyes of C57BL/6 male mice (18–20g). The corneal and limbal epithelia were removed by applying a rotary motion parallel to the limbus using a #21 blade (Feather, Osaka, Japan). After epithelial debridement, the animals were randomized to the treatment groups.

Corneal Neovascularization Quantitation

While deeply anesthetized, mice received 20 μg/g of fluorescein isothiocyanate-concanavalin A intravenously to label the vasculature. Thirty minutes later, mouse eyes were enucleated, fixed with 4% paraformaldehyde for 1 hour at 4°C, and the corneas were flat-mounted. Corneal NV was visualized using a DMRA2 (Leica, Deerfield, IL) epifluorescence microscope and quantified using Openlab imaging software (Improvision, Lexington, MA). Blood vessel area was quantified as follows. The perimeter of the entire corneal flat-mount was traced, followed by a tracing of the area in the middle of the cornea bounded by in-growing blood vessels. Subtraction of the inner corneal area from the entire corneal area provided a value for total blood vessel area. Blood vessel area is expressed as a percentage of corneal flat-mount area.

CNV Model

CNV was generated using a previously described technique[31] with the following modifications. Four burns were generated using diode laser photocoagulation (75-μm spot size, 0.1-s duration, 90 mW, Oculight SL laser; IRIDEX, Mountain View, CA) and a hand-held cover slide as a contact lens. Burns were localized to the 3, 6, 9, and 12 o'clock positions of the posterior pole of the retina. Formation of a bubble at the time of laser application indicates rupture of Bruch's membrane and is an important factor in successfully inducing CNV. Therefore, only those mice in which a bubble formed for all four laser burns were included in the study.

CNV Quantitation

Following enucleation of the eye, choroidal flat-mounts were obtained by removing the cornea and the lens and then peeling the neural retina away from the underlying retinal pigment epithelium. Radial cuts allowed the eyecup to be laid flat. Choroidal flat-mounts were fixed with 4% paraformaldehyde for 1 hour at 4°C and stained with either anti-PECAM-1 antibody or lectin as described below. Imaging of choroidal flat-mounts was performed as described for corneal flat-mounts. However, neovascularization was quantified by drawing a perimeter around areas of hyperfluorescence associated with each burn.

Morphometric Analysis

Retinal Blood Vessel Measurements

Images of retinal flat-mounts were acquired using a 20× objective. The vessel width and length was determined by drawing regions of interest on the image. The length in pixels was then converted to microns.

Corneal Thickness

Ten-micron sections of fixed cornea were imaged using a 20× objective. The thickness of the cornea was determined by drawing a region encompassing the width of the cornea on the image. Image analysis was performed using OpenLab software, Improvision).

Experimental Protocols

We used three different ocular neovascularization models to study the inhibition and regression of vessel growth. These are detailed below, and the protocols for each are summarized in Table 1.

Developing Retinal Vasculature Model

Neonatal mice were injected intraperitoneal daily with either 10 mg/kg of APB5, 50 mg/kg of anti-VEGF aptamer or both, starting on postnatal day 0 (P0). Mouse eyes were enucleated at two time points: postnatal day 3 (P3) and postnatal day 7 (P7, Table 1). For proliferation and apoptosis studies, eyes were enucleated at postnatal day 5 (P5).

Corneal NV Model

Both APB5 (at 5 mg/kg) and the anti-VEGF aptamer (at 25 mg/kg) were administered by intraperitoneal injection twice a day. In experiment 1, to study the effects of anti-angiogenic inhibitors on neovessel growth prevention, mice were treated with APB5 or anti-VEGF aptamer or both for 10 days immediately following injury at day 0 (D0). For experiment 2, to study the effects of anti-angiogenic inhibitors on vessel regression, mice were treated as above for 10 days starting at day 10 (D10) postinjury. In experiment 3, to assess how late in disease progression vessels could be regressed, mice were treated for 14 days starting at 14 days postinjury (D14, Table 1).

CNV Model

In experiment 4, for the vessel prevention study, mice were treated with APB5 or anti-VEGF aptamer or both for

Table 1. Experimental Protocols

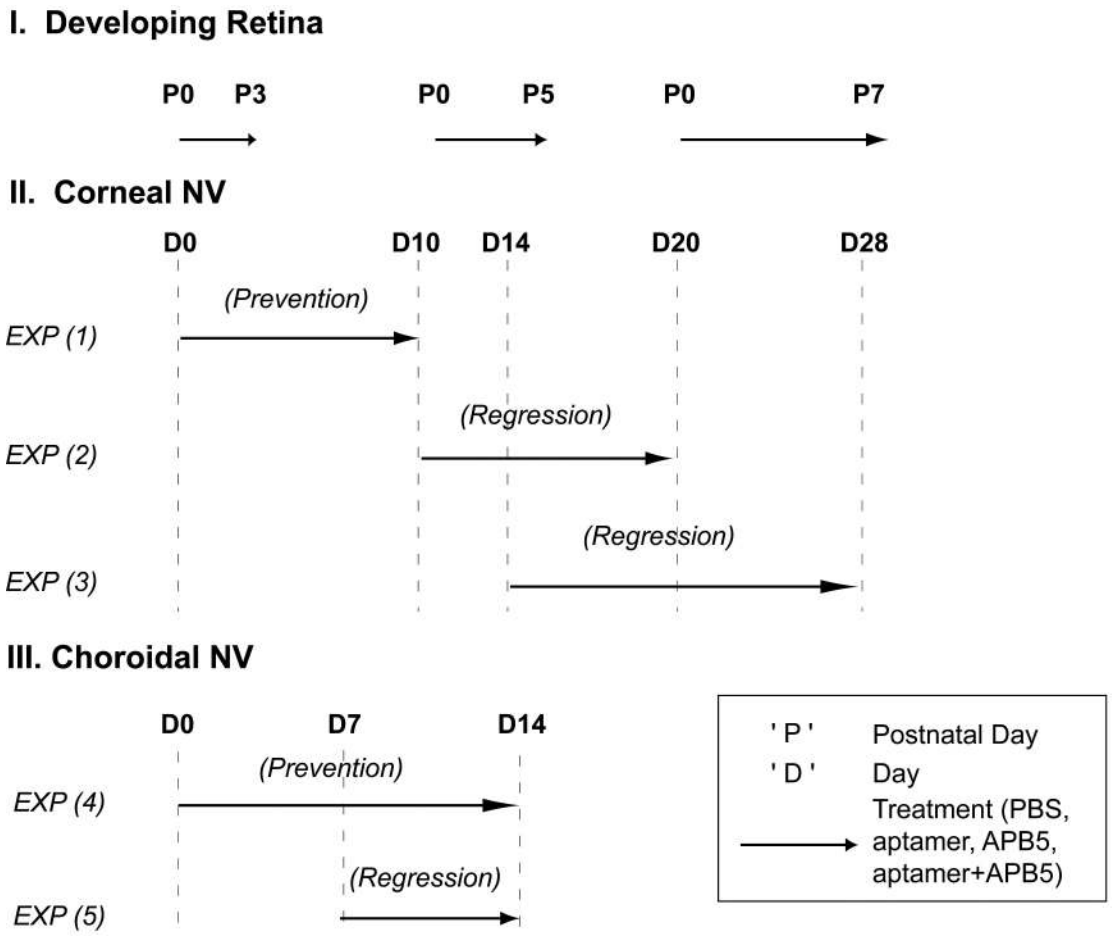

14 days immediately following laser injury. In experiment 5, for the regression study, mice were treated with APB5 or anti-VEGF aptamer or both for 7 days starting 7 days postlaser injury (Table 1). Mice injected with PBS alone served as controls.

Whole-Mount Immunofluorescence

Eyes were enucleated and fixed with 4% paraformaldehyde for 1 hour at 4°C. For whole-mount preparation, the retina and the cornea were exposed by removing other portions of the eye. After washing with PBS, tissues were placed in methanol for 20 minutes. Tissues were incubated overnight at 4°C with a primary antibody diluted in PBS containing 10% goat serum and 1% Triton X-100. Tissues were washed four times in PBS followed by incubation with a secondary antibody overnight at 4°C. Radial cuts were then made in the peripheral retina and cornea to allow flat mounting on a glass slide in mounting medium (Vectashield; Vector Laboratories). The flat-mounted tissues were examined by fluorescence microscopy.

Detection of Cell Proliferation and Apoptosis

Cells in the S phase of the cell cycle were labeled using anti-phospho-histone H3 antibody (PH3) by whole-mount immunostaining as described above. The flat-mounted tissues were examined by epifluorescence microscopy. Using a 5× objective, a 12-bit image of each quadrant of the retinal flat-mount was acquired and stored. PH3-positive cells were quantified by a masked observer as follows: the background of each image was flattened (Image J; National Institutes of Health, Bethesda, MD) and then an automatic threshold applied (threshold = average of image + (8 × SD)). Debris was excluded from the analysis by constraining the count of objects to a pre-determined pixel size representative of PH3-positive cells (Metamorph software; Universal Imaging Corp., Downingtown, PA).

To detect apoptotic cells, terminal deoxynucleotide transferase dUTP nick-end labeling (TUNEL) staining was used in cryosections of developing retina. For cryosection, eyes were frozen in OCT compound (Sakura Finetek, Torrance, CA) and sectioned at a thickness of 10

μm. TUNEL staining was performed with a fluorescein apoptosis detection system according to the manufacturer's instructions (Promega Corp., Madison, WI). To perform quantitative assessment of apoptotic ECs, the center of each eye was cut into 10-μm-thick sections. Ten sections spanning 500 μm were then stained with TUNEL and lectin for analysis. Because TUNEL-positive ECs in the superficial retinal vasculature cannot be captured in one focal plane, TUNEL-positive cells were counted manually by a masked observer. By manually moving around the inner layer of the retinal section and changing the focal plane, TUNEL-positive ECs were unambiguously detected and counted. The number of TUNEL-positive ECs was normalized to the total capillary area in the superficial layer, which was determined as follows. Multiple 12-bit grayscale images were captured of the lectin staining in the retinal cross-section using a 5× objective, and a composite image was created using Photoshop (Adobe, San Jose, CA). A region of interest that defines the superficial vasculature (~50 μm below the surface of the retina) was drawn on the composite image, and an automatic internal threshold was applied to the region. The sum of lectin-positive pixels was calibrated for area and used to normalize TUNEL-positive cells.

Histological Analysis and Electron Microscopy

Tissues were fixed with a mixture of 1.25% paraformaldehyde, 2.5% glutaraldehyde in 0.1 mol/L sodium cacodylate, pH 7.4. Select areas were cut from each quadrant, placed in 0.2 mol/L sodium cacodylate rinse (3×, 10 minutes), postfixed in 1% osmium tetraoxide/0.1 mol/L sodium cacodylate for 60 to 90 minutes, and rinsed again as above. Tissue was dehydrated through 50%, 70%, 95%, and 100% acetone before infiltration with acetone: fresh Spurrs resin (2:1), then the same mixture at 1:2, and finally 100% Spurrs resin overnight. Tissues were embedded between Transwell polyester membranes and polymerized in the oven overnight at 60°C. Semithin sections were cut with a diamond knife on a Leica Ultracut and stained with 0.5% Toluidine Blue in 0.1% sodium borate; micrographs were captured on a Leica DMRA2 wide field microscope. 70 to 100 nm tissue sections were stained with 0.5% uranyl acetate (aqueous) followed by Reynolds lead citrate. Sections were analyzed with a transmission electron microscope (model 1010; JEOL, Tokyo, Japan), and images were captured with an AMT digital capture system (Advanced Microscopy Techniques Corp., Danvers, MA). Electron micrographs of capillary cross-sections were captured whenever an intact capillary was found in the section. EC/pericyte association was quantified by three trained, masked observers who classified each capillary into one of three groups: naked capillaries, capillaries with pericyte attached, and undetermined.

RNA Isolation and Quantitative RT-PCR Analysis

Quantitative evaluation of mouse VEGF-A, PDGF-B, and PDGFR-β expression after corneal injury was assessed by real-time quantitative RT-PCR using a sequence detection system (TaqMan Chemistry and GeneAmp 7900HT; Applied Biosystems, Forest City, CA). Cornea samples were collected in a cell lysis solution from Qiagen Inc. (Valencia, CA) containing β-mercaptoethanol. RNA was isolated following RNeasy mini kit protocols (Qiagen Inc.) and transcribed into single-stranded cDNA using Multiscribe Reverse Transcriptase (Applied Biosystems). Real-time quantitative RT-PCR analysis was performed using custom primers (Applied Biosystems) for VEGF-A, PDGF-B, and PDGFR-β and for glyceraldehyde-3-phosphate dehydrogenase as an internal control. Gene expression was quantified using the Comparative C_T Method.[32] Concentration of anti-VEGF aptamer in tissues was determined by dual hybridization as described (Patent Application Serial No. 11/186,660).

Statistical Analysis

All values are expressed as mean ± SE analysis of variance followed by a post hoc Bonferroni test used to determine the significance of differences in multiple comparisons. Differences with a value of $P < 0.05$ were considered significant.

Results

MCs Provide Vessel Stability When VEGF-A Levels Are Compromised

MCs are recruited to all developing retinal vessels.[18] However, MCs exhibit distinct immunochemical and histological features that are dependent on the types of vessels with which they associate. We chose NG2 as an MC marker in our experiment, because NG2-positive MCs (Figure 1A) were also positive for PDGFR-β (Figure 1B) and were located around all vessels of the developing retina. We found that injection of the anti-PDGFR-β antibody, APB5 (10 mg/kg daily), prevented MC recruitment to ECs on almost all developing blood vessels of the retina in agreement with previous reports.[33] We could only detect NG2-positive cells in the roots of a few large vessels (Figure 1C). In contrast, mice receiving the same injection protocol but with PBS presented a normal vasculature (Figure 1C).

Having established a protocol for generating retinal blood vessels that lack MCs, we tested the hypothesis that the efficacy of anti-VEGF inhibition may be different on blood vessels covered with MCs compared with naked blood vessels. We injected neonatal mice daily from birth (postnatal day 0, P0) with the anti-VEGF aptamer, APB5 antibody, aptamer and APB5 in combination, or PBS as a control. The anti-VEGF aptamer did not significantly affect the growth of retinal vasculature or MC recruitment to retinal vessels, as compared to PBS controls (Figure 2, A and B). This is in contrast to the reported activity of pan-VEGF inhibitors and is likely due to the specificity of the aptamer for a subset of VEGF isoforms.[29] Injection of APB5, however, significantly reduced MC recruitment to the developing vessels of the retina. In addition, vessel growth was impaired at P3

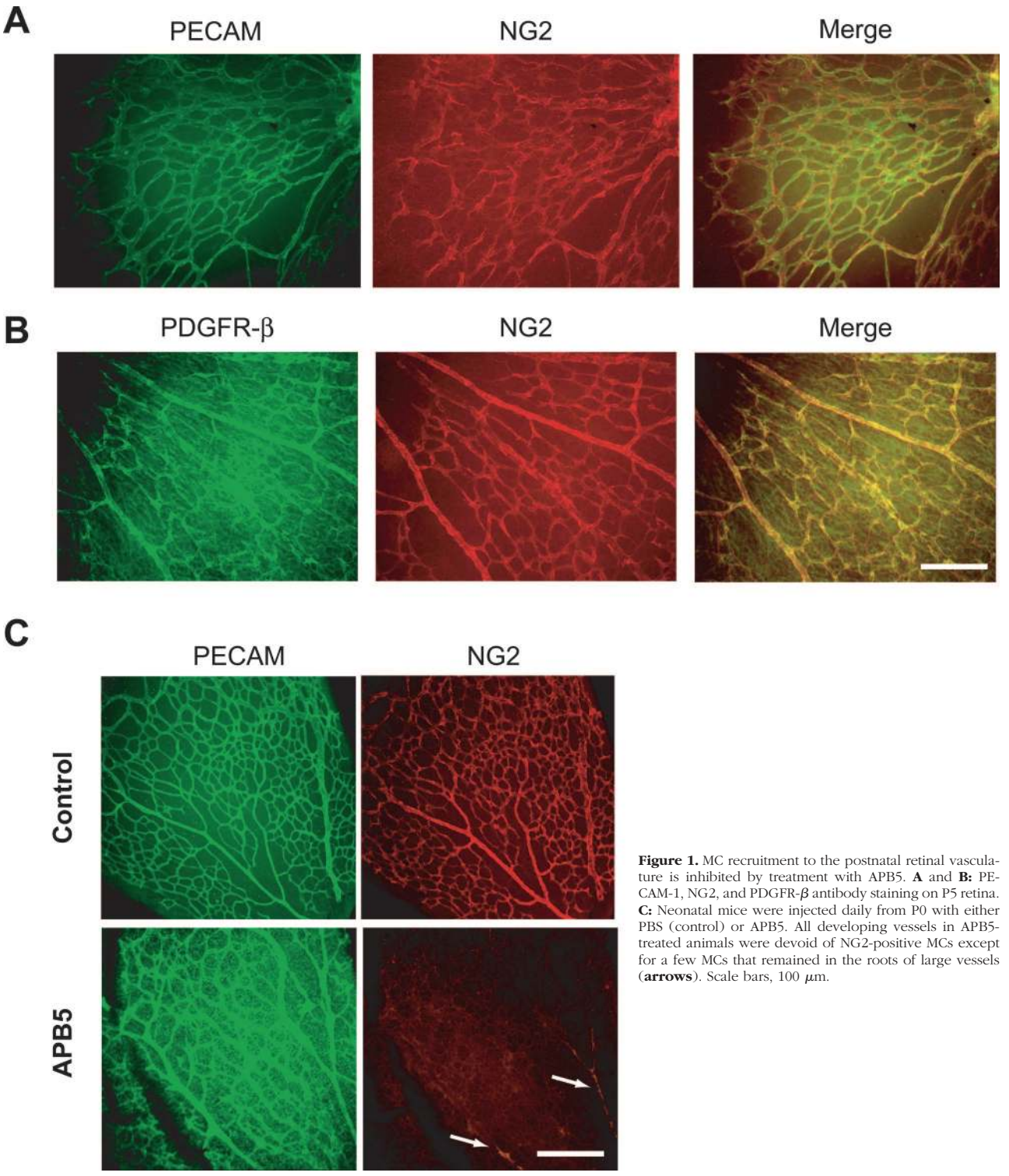

Figure 1. MC recruitment to the postnatal retinal vasculature is inhibited by treatment with APB5. **A** and **B:** PECAM-1, NG2, and PDGFR-β antibody staining on P5 retina. **C:** Neonatal mice were injected daily from P0 with either PBS (control) or APB5. All developing vessels in APB5-treated animals were devoid of NG2-positive MCs except for a few MCs that remained in the roots of large vessels (**arrows**). Scale bars, 100 μm.

(Figure 2, A and B), and abnormal vasculature with enlarged vessels was observed at P7 as compared to the retina of PBS-injected controls (Figure 2, C and D). Impaired MC recruitment following the inhibition of PDGF-B signaling has been previously shown to result in vessel enlargement.[17,18] When mice were treated with both the anti-VEGF aptamer and APB5, inhibition of vessel growth was significantly greater than in mice treated with either agent alone (Figure 2, A and B). In mice treated with this combination therapy, the P7 retinal vessels were severely enlarged (Figure 2, C and D). We speculated that the abnormality in the growing vasculature could be due to hyperproliferation (vessel enlargement) and/or apoptosis of ECs (reduced vascular area). We analyzed proliferation and apoptosis of ECs in all experimental groups at P5, a mid-point between the observed vascular area

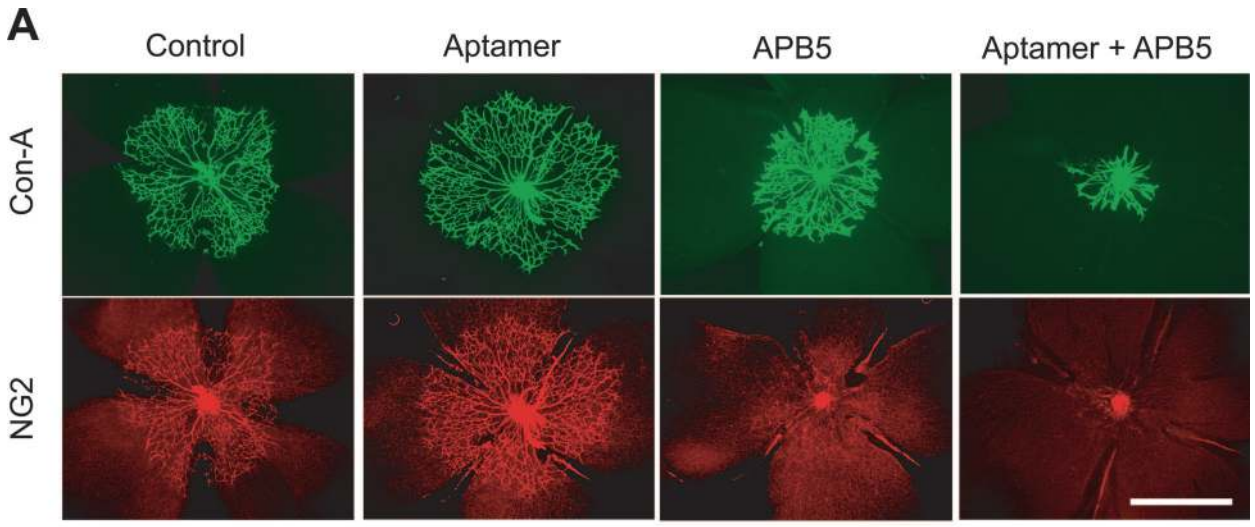

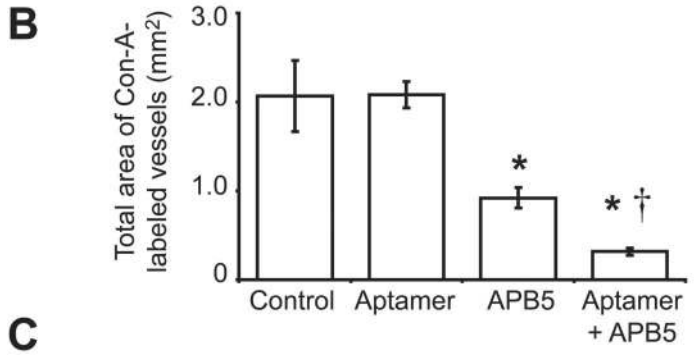

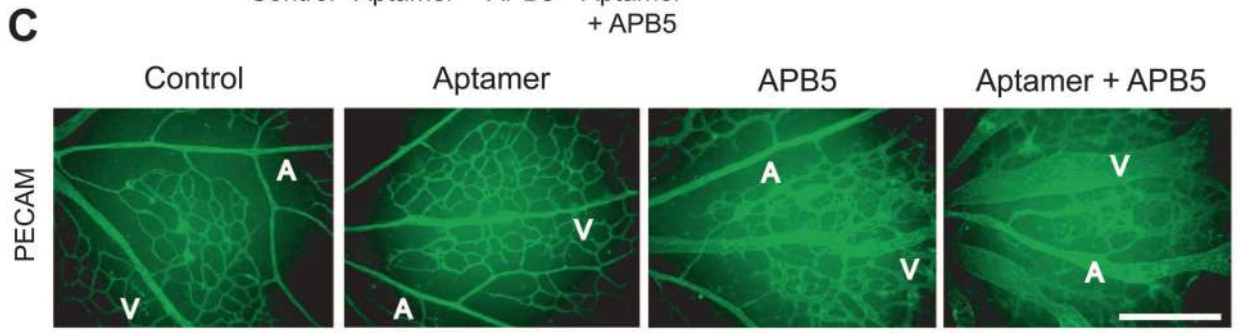

D

Characteristics of retinal vessels

	Control	Aptamer	APB5	Aptamer + APB5
Length of vessels (mm)	2.2 ± 0.05	2.09 ± 0.04	1.89 ± 0.03 *	1.69 ± 0.06 *†
Width of arterioles (μm)	12.6 ± 0.67	13.6 ± 0.51	21.0 ± 1.78 *	33.3 ± 1.54 *†
Width of venules (μm)	28.1 ± 1.68	26.4 ± 2.91	45.3 ± 5.49 *	88.2 ± 10.1 *†

Figure 2. Blocking VEGF-A and PDGF-B signaling affects retinal vascular growth and morphology. Neonatal mice were injected daily with anti-VEGF aptamer or APB5 or both. **A:** P3 retinal vessels in each treatment group were labeled by perfusion with concanavalin A (green) and then immunostained for NG2 (red). Scale bar, 500 μm. **B:** Quantification of the total vessel area in the P3 retina. **C:** P7 retinal vasculature was labeled with PECAM-1 staining. Scale bar, 100 μm. **D:** Analysis of P7 retinal vessel length and width. $^{*}P < 0.01$ compared to control or anti-VEGF aptamer-treated mice; $^{\dagger}P < 0.05$ compared to APB5-treated mice.

reduction (P3) and the subsequent severe tissue disruption (P7). To detect proliferating cells, we used an antibody against PH3. The number of PH3-positive ECs was not significantly different in the treated and control retinas (Figure 3, A and B). We observed few PH3-positive ECs in the enlarged vessel areas present in APB5/anti-VEGF

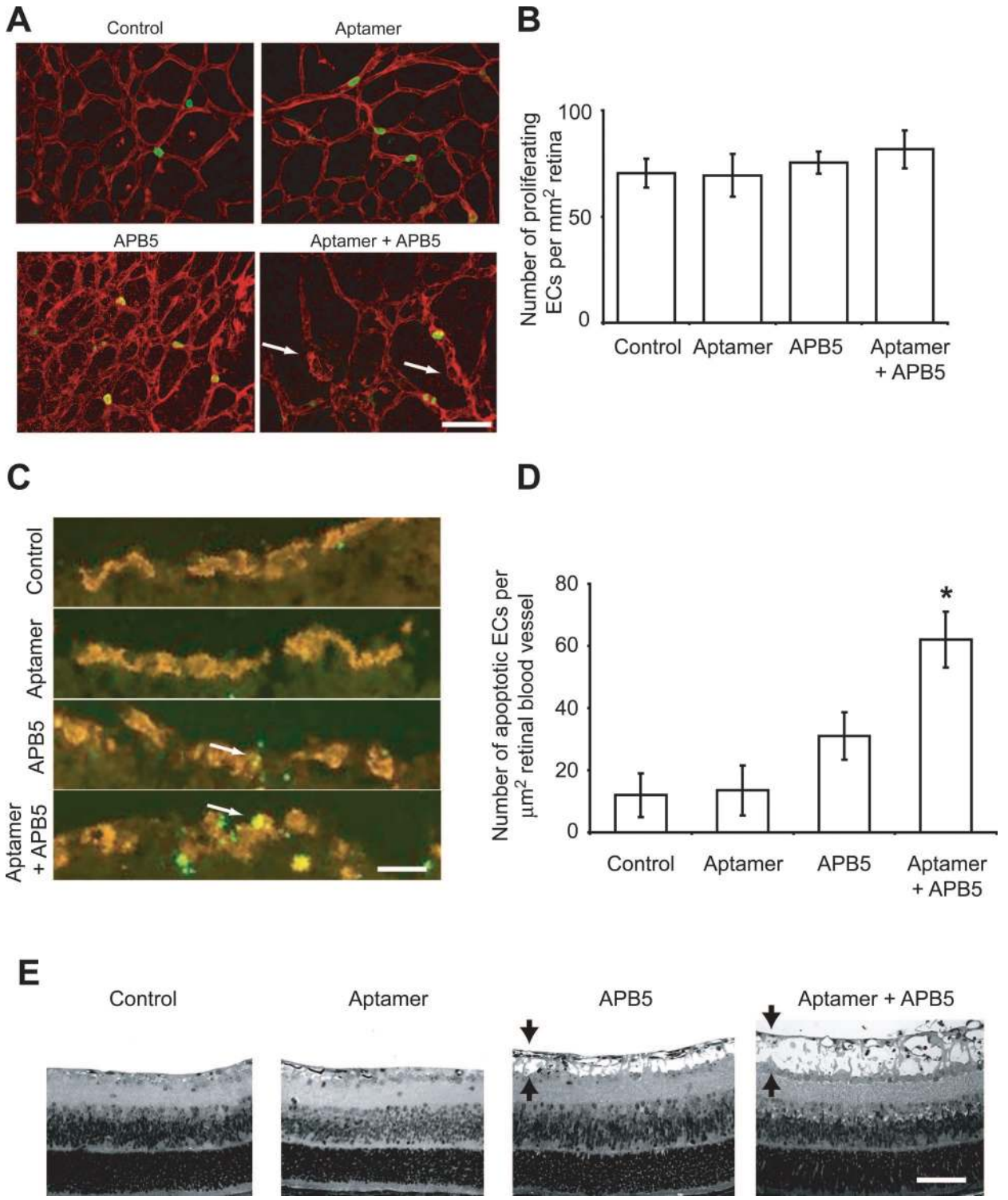

Figure 3. Change in EC proliferation and apoptosis following combination therapy. **A:** Double labeling with PH3 (green) and lectin staining (red) of P5 retina in each treatment group. In the APB5-treated and combination-treated samples, the distribution of PH3-positive ECs observed is similar to control samples. Enlarged regions in vessels (**arrows**) did not correlate with an increase in PH3-positive ECs. Scale bar, 100 μm. **B:** Quantitation of proliferating ECs in PBS control and treatment groups. **C:** Detection of apoptotic ECs by double labeling with TUNEL (green) and lectin staining (red). **Arrows**, apoptotic ECs. **D:** Quantitation of apoptotic ECs in control and treatment groups. **E:** 0.5-μm sections of P7 retina from each treatment group showing retinal edema in both the APB5 and the combination samples. Scale bar, 50 μm.

aptamer-treated retinas, suggesting that these aneurysms and abnormalities were not caused by an increase in EC proliferation but were primarily the result of altered EC shape and organization, as previously reported.[34] In contrast, the number of apoptotic ECs in mice treated with combination therapy was significantly higher than in

other experimental groups (Figure 3, C and D), providing a possible explanation for the much reduced vascular area present in this group. In addition, we observed that the APB5- and combination-treated group presented edema in the inner retina (Figure 3E). This edema could be caused by the effect of PDGF-B signaling inhibitors on the vasculature or on retina tissue development.

Inhibition of PDGF-B Signaling in Corneal NV Prevents MC Recruitment to Nascent Vessels and Induces MC Drop-out in Older Vessels

Most ocular pathologies are associated with abnormal vessel growth. Thus, we wanted to evaluate the effect of combination therapy on pathological blood vessels in the eye. Abnormal vessel growth into the avascular cornea occurs as a response to epithelial debridement (Figure 4A). Blood vessels grow mostly in the first 7 days postinjury and minimally thereafter (Figure 4B). Importantly, the cornea remains vascularized even 28 days after epithelium debridement without natural regression, making the cornea model suitable for studying pharmacological approaches aimed at vessel regression. By day 10 postinjury, vessels were completely covered with SMA-, NG2-, and PDGFR-β-positive MCs (Figure 4, C–E). On day 10 postinjury, VEGF-A, PDGF-B, and PDGFR-β expression was significantly elevated (Figure 4F).

We tested whether blocking PDGF-B signaling would interfere with MC recruitment to corneal neovessels. Indeed, we found that, in our model of corneal NV, treatment with the anti-PDGFR-β antibody APB5 results in significantly less MC recruitment to nascent vessels (days 0 to 10) compared to control PBS injection (Figure 5A). To investigate whether MCs could be stripped from 10-day-old corneal vessels (days 10 to 20; Figure 5B) mice were injected with APB5 for 10 days starting 10 days postinjury (for experimental design see Table 1). Indeed, the MC coverage of these vessels was greatly reduced, and new vessels grew devoid of MCs in APB5-treated mice compared to day 20 controls. In general, MCs appeared to detach from corneal neovessels following APB5 treatment, whereas MCs covered all pathological vessels more uniformly and tightly in PBS controls. However, the limbal vessels in the corneal NV model remained covered with MCs in both the APB5-treated and PBS control mice (Figure 5C). Therefore, inhibition of PDGF-B signaling only affects the new vessels that grow as a result of epithelial debridement.

We based our observations about MC behavior following PDGF-B signaling inhibition on the SMA expression pattern. However, changes in the pattern of SMA staining may simply reflect changes in MC marker expression profile and not changes in the number of MCs present. Indeed, it has been previously reported that MC marker expression is very heterogeneous in some angiogenic conditions, with MCs known to express different markers in different tumor settings.[33] To confirm that MC marker loss indeed reflected an absence of MCs following PDGF-B signaling inhibition, we performed ultrastructural analysis of new vessel profiles after APB5 treatment. New vessel profiles were classified based on the following categories: 1) naked capillary, 2) capillary with attached pericyte, and 3) undetermined (Figure 6A). In control samples, 84.2% of vessels had pericytes attached to them, whereas in APB5-treated samples only 42.9% of vessels showed EC/pericyte association (Figure 6B). More than half of the vessels (56.6%) counted were naked capillaries in APB5-treated samples as compared to only 12.7% in controls. Therefore, the EM quantitation is in agreement with the pericyte loss observed following APB5 treatment as visualized by SMA staining (Figure 5C).

Combination Therapy Is More Effective Than Mono-therapy at Causing Vessel Regression in the Corneal NV Model

We have shown that blocking PDGF-B signaling using different inhibitors leads to altered MC recruitment to nascent vessels and the detachment of MCs from 10-day-old vessels in the corneal NV model. We wanted to investigate whether MC removal would affect neovessel growth and survival in the presence of anti-VEGF treatment. Mice were treated with APB5 or anti-VEGF aptamer or both immediately following corneal injury for 10 days. Control animals received PBS injections. Mice treated with the anti-VEGF aptamer had a substantial decrease in the area of NV (Figure 7), underscoring VEGF-A inhibition as an effective therapy for the prevention of new blood vessel growth. Treatment with APB5 alone minimally affected development of NV (Figure 7A). Mice treated with both APB5 and anti-VEGF aptamer showed additional benefit with a smaller NV area than all other treatment groups (Figure 7B). Thus, anti-VEGF treatment is effective at preventing new vessel growth but less so than anti-VEGF and anti-PDGF treatment combined.

We wished to explore whether both anti-VEGF and combination therapy remained effective over time. Therefore, we tested anti-VEGF and anti-PDGF reagents on 10- and 14-day-old cornea vessels. We chose these time points based on the fact that, in the corneal NV model, neovessel growth slows down from day 10 onward (Figure 4B). Mice were treated with a PDGF-B signaling inhibitor or anti-VEGF aptamer or both, at 10 days postinjury for 10 days (until day 20, see Table 1). Both APB5 and Gleevec were used as PDGF-B signaling inhibitors in this experiment and behaved similarly (APB5 data shown). Treatment with the anti-VEGF aptamer did not affect vessel composition (Figure 8A) but inhibited vessel growth as compared to day 20 PBS control mice (Figure 8B). However, there was no significant vessel regression in anti-VEGF-treated mice compared to day 10 controls (represented as 0 on the *y* axis, Figure 8B), suggesting that blocking VEGF signaling was sufficient to prevent neovessel growth but unable to cause vessel regression. In APB5-treated mice, MCs were stripped from 10-day-old corneal vessels, leaving mostly bare EC tubes compared to controls (Figure 8A). The total area occupied by naked NV, however, was comparable to that of day 20 PBS controls (Figure 8B) confirming that MC depletion

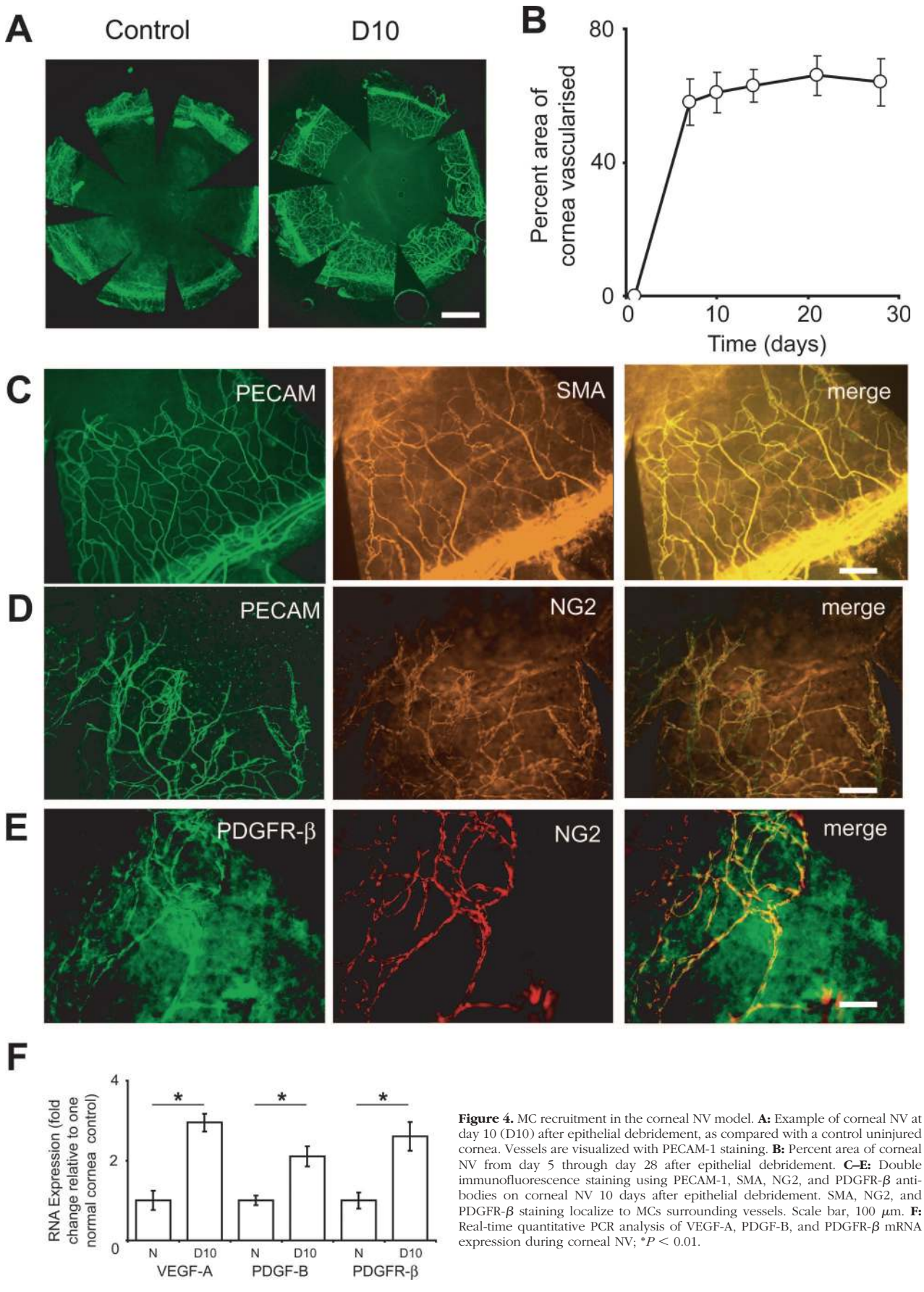

Figure 4. MC recruitment in the corneal NV model. **A:** Example of corneal NV at day 10 (D10) after epithelial debridement, as compared with a control uninjured cornea. Vessels are visualized with PECAM-1 staining. **B:** Percent area of corneal NV from day 5 through day 28 after epithelial debridement. **C–E:** Double immunofluorescence staining using PECAM-1, SMA, NG2, and PDGFR-β antibodies on corneal NV 10 days after epithelial debridement. SMA, NG2, and PDGFR-β staining localize to MCs surrounding vessels. Scale bar, 100 μm. **F:** Real-time quantitative PCR analysis of VEGF-A, PDGF-B, and PDGFR-β mRNA expression during corneal NV; $^*P < 0.01$.

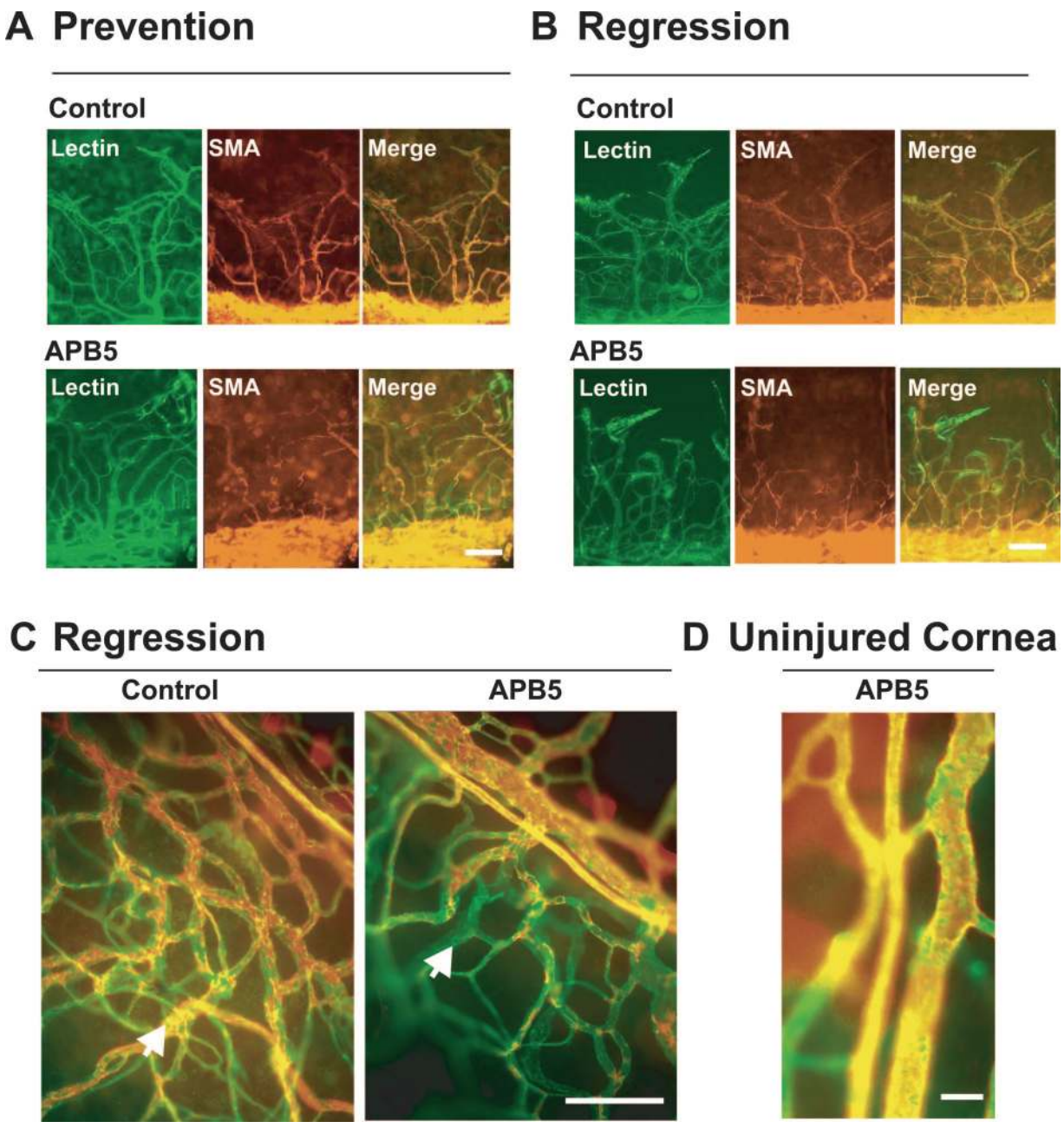

Figure 5. Inhibition of PDGF-B signaling blocks MC recruitment and results in MC stripping of corneal neovessels. **A–C:** ECs were labeled by staining with lectin (green) and MCs by staining with SMA (red) in all samples. **A:** Prevention: Corneal NV was induced on D0, and mice were treated daily with APB5 until D10 postinjury. MC recruitment to new vessels was reduced by treatment with APB5 compared to PBS controls (see SMA panels). **B** and **C:** Regression: To test whether treatment was as effective at later times, mice were injected with APB5 every day starting 10 days postinjury for 10 days and sacrificed 20 days postinjury. Scale bar, 100 μm. **B:** MC vessel coverage was reduced in mice treated with APB5 as compared to D20 PBS controls. **C:** High magnification images of corneas from injured mice treated from D10 to D20 with either PBS or APB5. Neovessels in PBS controls had greater MC coverage than in APB5-treated animals (**arrowheads**). Scale bar, 20 μm. **D:** The limbus of uninjured animals remained covered by MCs despite treatment with APB5 from D10 to D20. Scale bar, 5 μm.

alone did not significantly affect vessel growth. In corneas from animals treated with combination therapy, the population of MC-covered vessels decreased as in mice treated with APB5 alone, but in addition, few MC-free vessels were observed (Figure 8A). Thus, we observed a significant decrease in new vessel growth in combination-treated mice compared to day 20 PBS control mice and significant regression compared to day 10 PBS controls (Figure 8B).

Similar results were observed in animals where treatment was initiated later, at day 14, and continued until day 28 (see Table 1). The anti-VEGF aptamer alone showed inhibition of neovessel growth compared to day 28 control mice but did not show regression as compared to day 14 PBS controls (represented as 0 on the *y* axis, Figure 8C). The inhibition of neovessel growth observed in the day 14 to 28 treatment period was less significant than that observed when anti-VEGF treatment was ad-

A

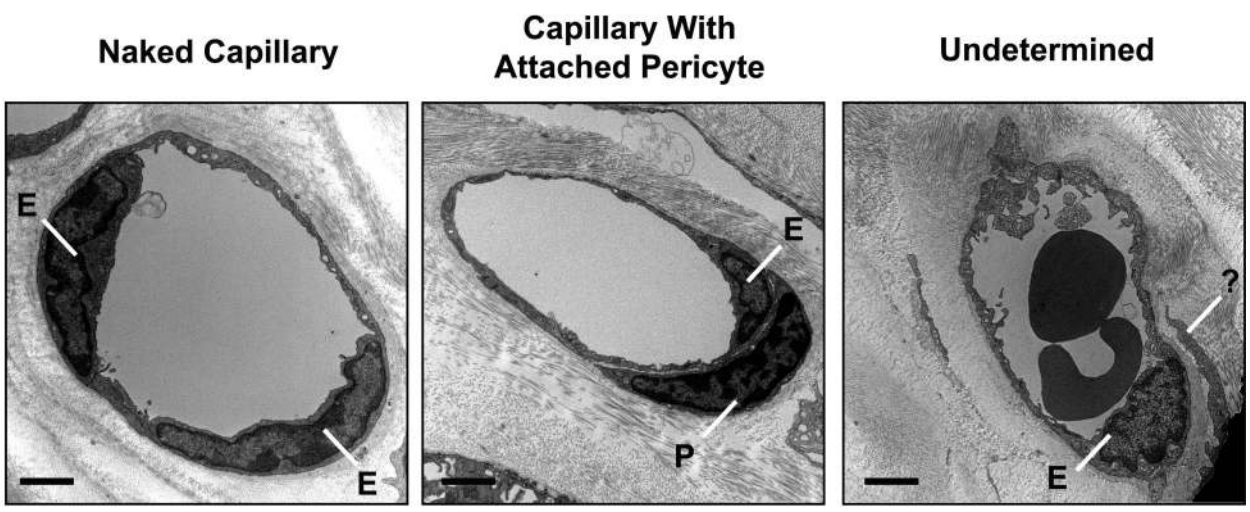

B Quantification of pericyte association with ECs

	Control (313)	APB5 (263)
Naked capillary	12.7	56.6
Capillary + pericyte	84.2	42.9
Undetermined	3.1	1.5

Values represent percentage of images for each category; numbers in parentheses are total images analyzed

Figure 6. EC/MC association is reduced in cornea neovessels of mice treated with APB5 as revealed by electron microscopy. **A:** Electron micrographs were divided into three groups (representative images for all groups were taken from D0 to D10 APB5-treated samples): naked Capillary, capillary with attached pericyte and undetermined; E, endothelial cell; P, pericyte; ?, unidentified cell structure. Scale bar, 2 μm. **B:** The percentage of pericyte association with ECs is shown.

ministered from day 10 to 20 (compare aptamer-treated group in Figure 8, B and C) suggesting reduced efficacy of anti-VEGF therapy over time. In contrast, mice treated with combination therapy from day 14 postinjury until day 28 had not only inhibition of new vessel growth compared to PBS injected control mice but also significant vessel regression compared to day 14 PBS controls (Figure 8C).

Our results on the developing retina and in previous reports[11,23] suggest that combination therapy might induce edema. We explored whether combination therapy increased edema in the corneal NV model by measuring corneal thickness. As expected neovascular growth causes thickening of the cornea, but there was no significant increase in corneal thickness in either anti-VEGF aptamer or combination therapy-treated animals as compared to untreated controls (Figure 8D).

Although anti-VEGF therapy resulted in reduced corneal NV, there was a marked decrease in its effectiveness over time in this model (Figure 8, B and C), in agreement with observations made in other systems.[11,23] We explored whether this decrease in effectiveness was related to a decrease in the amount of anti-VEGF aptamer present in the cornea over time. We conducted a separate experiment to correlate the extent of neovascular inhibition at different time points with the amount of anti-VEGF aptamer in the cornea. We found that, although the extent of inhibition of neovascularization decreased with time (Figure 9A), the amount of anti-VEGF aptamer increased slightly with time (Figure 9B). Thus, concentrations of anti-VEGF aptamer that were sufficient to inhibit vessel growth between days 0 and 10 were less effective at inhibiting the growth of vessels between days 10 and 20 or days 20 and 30. The effectiveness of combination therapy was also found to diminish over time in this model, but at each time it remained more efficacious than anti-VEGF aptamer alone (Figure 9C).

Combination Therapy Is Effective in CNV

Abnormal growth of choroidal vessels is one of the hallmarks of age-related macular degeneration that can be studied in the laser-induced CNV mouse model.[5] Because we are interested in developing and improving therapeutics for the treatment of age-related macular degeneration, we tested the effectiveness of our combination approach in murine CNV. In a prevention study, CNV was induced by laser injury, and subsequently animals were treated with APB5 or anti-VEGF aptamer or both for 14 days. Mice treated with APB5 alone had neovascular lesions of similar area as PBS-injected control mice (Figure 10A). In contrast, mice treated with the anti-VEGF aptamer had a statistically significant decrease in the area of NV (Figure 10A). However, mice treated with the anti-VEGF aptamer and APB5 exhibited the smallest NV lesions as compared to all other treatment groups (Figure 10A).

To evaluate its efficacy on older lesions, we treated 7-day-old CNV with combination therapy. Laser injury was performed at day 0, and treatment started 7 days postinjury for 7 days (see Table 1); vessel growth was measured 14 days postinjury. Treatment with APB5 had

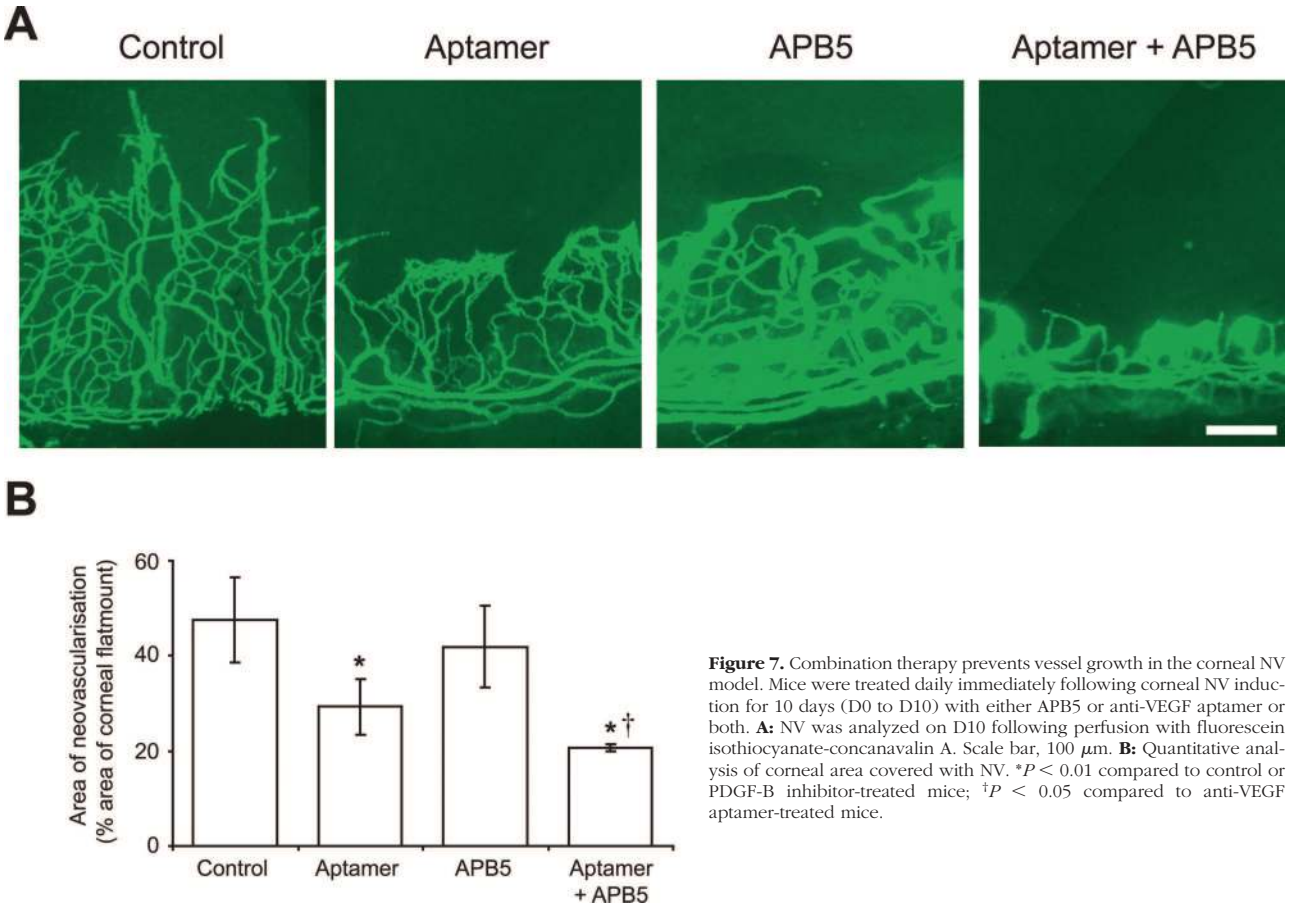

Figure 7. Combination therapy prevents vessel growth in the corneal NV model. Mice were treated daily immediately following corneal NV induction for 10 days (D0 to D10) with either APB5 or anti-VEGF aptamer or both. **A:** NV was analyzed on D10 following perfusion with fluorescein isothiocyanate-concanavalin A. Scale bar, 100 μm. **B:** Quantitative analysis of corneal area covered with NV. $^{*}P < 0.01$ compared to control or PDGF-B inhibitor-treated mice; $^{\dagger}P < 0.05$ compared to anti-VEGF aptamer-treated mice.

no effect on lesion size compared to PBS control (Figure 10B). However, mice treated with anti-VEGF aptamer had a statistically significant decrease in lesion area compared to PBS injected control mice (Figure 10B). The most dramatic inhibition of CNV was observed when mice were treated with both anti-PDGF-B and anti-VEGF inhibitors, underscoring the effectiveness of blocking both pathways rather than either of them separately (Figure 10B).

Discussion

In the present study, we show that blocking PDGF-B signaling enhances the effect of anti-VEGF therapy in three ocular models: developmental angiogenesis, corneal NV, and CNV. Blocking both VEGF-A and PDGF-B signaling pathways is superior to mono-therapy in the prevention of corneal and CNV and, furthermore, can cause regression of VEGF-independent vessels in these models. This report presents the first evidence for pharmacological combination therapy as a viable approach for the treatment of ocular angiogenesis.

VEGF-A is a known regulator of angiogenesis and permeability. Targeting VEGF-A has been recently validated in clinical trials as an effective therapy for diseases associated with pathological angiogenesis.[35–37] However, there are limitations to anti-VEGF therapy both in oncology[13] and ophthalmology, reflecting perhaps a change in vessel dependence on VEGF-A with time.[11,12] Indeed, we found the effectiveness of anti-VEGF treatment in causing vessel regression decreased over time in our animal model of corneal NV (Figures 8 and 9).

Ocular diseases associated with deregulated vessel growth develop over long periods of time, and, therefore, effective treatment would target not only the actively growing vasculature but also pre-existing pathological vessels. Thus, intervention should aim to target vessel regression for maximum clinical effect. Since some animal models of ocular NV present natural vessel regression over time,[6,38] we explored using the corneal NV model for neovascular regression. We determined this model to be optimal for the study of vessel regression, because corneal neovessels do not regress naturally for up to 4 weeks following injury.[39]

Although the developmental processes underlying new blood vessel formation and maturation have been well studied,[40] many questions still remain regarding what constitutes a 'mature' or established vessel. Vessel maturity has been linked to both the presence of MCs and a reduced dependence on VEGF-A for survival.[11,12]

The mechanisms leading to vessel maturity and VEGF-A independence are still poorly understood. Generally, it is thought that blood vessels require VEGF-A during embryonic development and at sites of natural adult blood vessel growth settings such as bone and

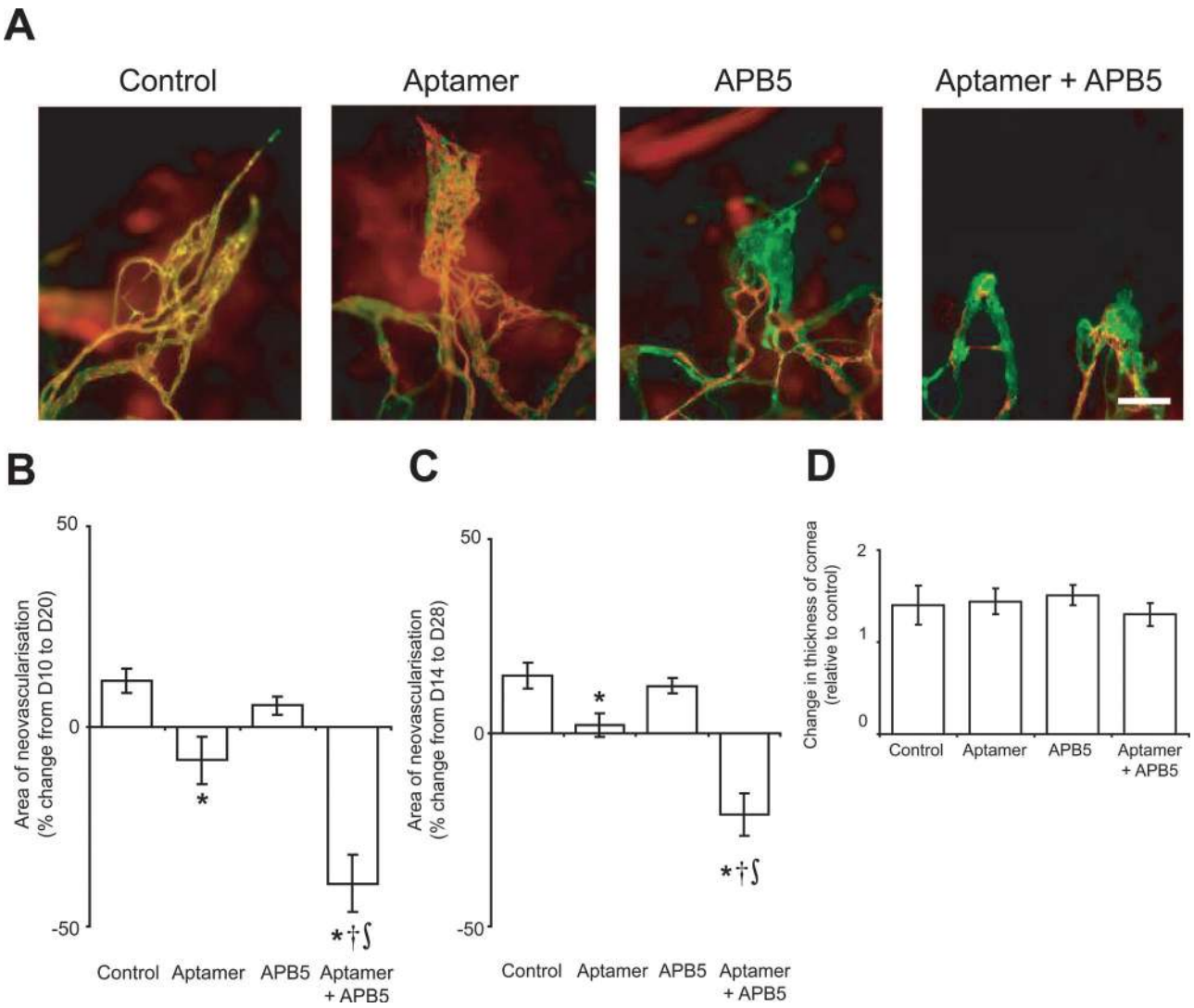

Figure 8. Combination therapy caused vessel regression over time. **A** and **B:** Treatment of corneal NV started at 10 days postinjury for 10 days (D10 to D20). **A:** Vessels were visualized by perfusion with fluorescein isothiocyanate-concanavalin A, and MCs were stained with SMA (red). Scale bar, 100 μm. **B:** Quantitative analysis of neovascular regression expressed as the percent change in NV area at D20 (after 10 days of treatment) compared to D10 (before treatment; represented as 0 on the y axis). $^{*}P < 0.05$ compared to D20 control or PDGF-B inhibitor-treated mice; $^{\dagger}P < 0.01$ compared to anti-VEGF aptamer-treated mice. $^{\int}$, $P < 0.01$ compared to D10 mice (before treatment). **C:** In this experiment treatment was started 14 days postinjury until D28 (D14 to D28). Quantitative analysis of NV regression expressed as the percentage change in NV area as compared to D14 (before treatment). $^{*}P < 0.05$ compared to D28 control mice; $^{\dagger}P < 0.01$ compared to anti-VEGF aptamer-treated mice. $^{\int}P < 0.01$ compared to D14 mice (before treatment). **D:** Injured corneal thickness was determined by measuring cornea width in sections of control and treated eyes. Data are expressed as -fold change to normal (uninjured) corneal thickness.

reproductive angiogenesis.[41,42] Pathological vessels resulting from aberrant angiogenesis in the adult are highly dependent on VEGF-A, although there is mounting evidence of pathological vessel resistance to anti-VEGF therapy.[12,13]

Although VEGF-A is the primary regulator of blood vessel growth, other pathways such as PDGF-B signaling regulate the process of EC/MC association, a necessary, but not sufficient, step in vessel stabilization.[14–16] Transgenic mice lacking PDGF-B/PDGFR-β fail to recruit MCs during embryonic vessel development,[15–17] as did treatment of the developing retina with a PDGFR-β blocking antibody, causing severe edema and blood vessel abnormalities. Little is known, however, about the effect of blocking PDGFR-β on MC recruitment to angiogenic vessels in adult tissues. In the present study, we first describe that corneal neovessels are associated with MCs as defined by the expression of a variety of MC markers. This evaluation is essential because the study of MCs and their contribution to vessel function has been hindered, in part, by the difficulty in identifying these cells due to the fact that specific marker expression can vary markedly in different tissues and vascular beds.[11,12] For example, angiogenic tumor vessels can be associated with populations of MCs that differ in their marker expression profiles over time.[14,33] Ultimately, it is a combination of their distinctive morphology and perivascular localization together with the expression of specific markers such as SMA, NG2, desmin, and PDGFR-β[43–45] that determines the presence of MCs. In our ocular NV models, we show that the absence of pericyte marker

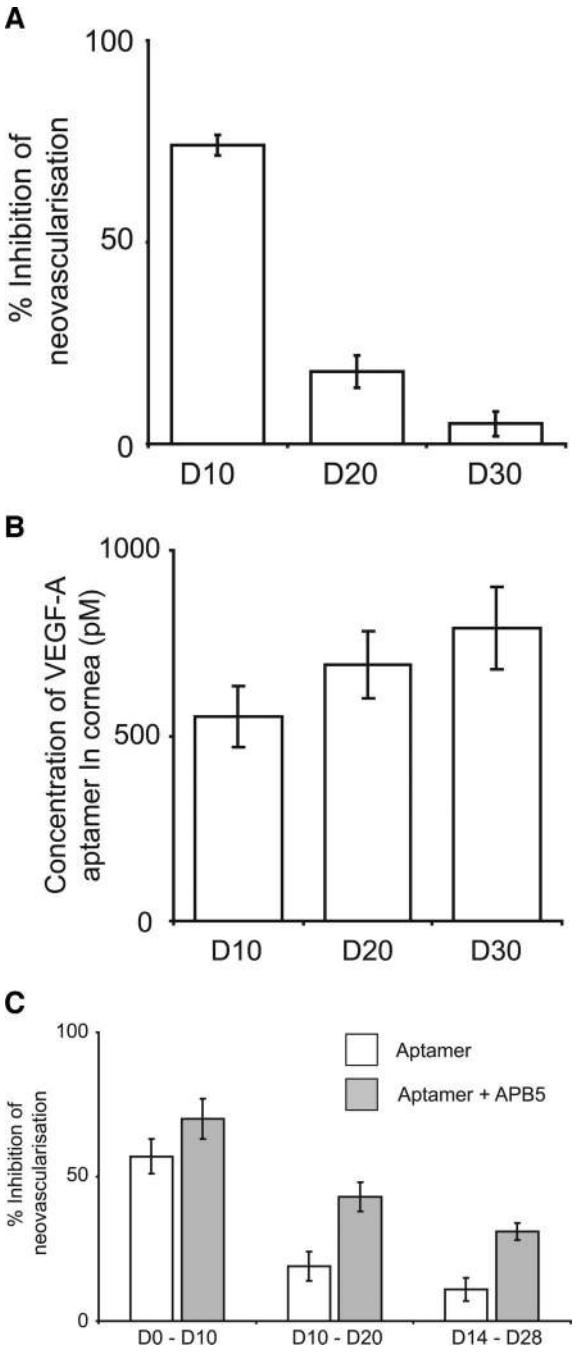

Figure 9. The efficacy of the anti-VEGF aptamer diminishes over time. Animals were treated at different times postinjury from D0 to D10, D10 to D20, or D20 to D30. **A:** One cornea from each treated animal was stained (with PECAM-1) for neovessel quantitation; the other cornea was processed for determination of anti-VEGF aptamer tissue concentration using a dual hybridization assay (**B**). $n = 4$ animals per experimental group. **C:** Combination therapy is more effective over time than anti-VEGF inhibition alone.

expression indeed correlated with pericyte loss in agreement with recent studies examining pericyte marker expression in tumor vessels.[46]

A previous study using the RIPTag2 pancreatic islet tumor mouse model demonstrated that combined targeting of VEGF-A and PDGF-B signaling using RTK inhibitors disrupted the association of MCs with ECs, reduced the tumor vascularity, and resulted in greater inhibition of tumor growth compared with targeting VEGF-A signaling alone.[22] We have expanded on these findings using neovascularization models that allow detailed cell biology analysis without the complexity of tumor settings and are able to demonstrate that the disruption of the EC/MC association occurs directly as a consequence of blocking PDGF-B signaling rather than as a result of tumor growth inhibition. Furthermore, RTK inhibitors are known to act on a broad range of kinases, making it difficult to rule out effects observed due to the inhibition of kinases other than PDGFR-β. We have used specific inhibitors of VEGF-A and PDGFR-β to show that the effects observed on MC/EC interactions are due to the specific inhibition of PDGF-B signaling.

In vessels of the developing retina, and even in the established neovessels of the cornea and CNV models, inhibition of PDGFR-β signaling resulted in pericyte depletion. In addition, PDGF-B inhibition alone resulted in edema and abnormal vessel morphology in the developing retina but not in the cornea NV model (compare Figure 3, A and E, with Figure 8D). The retinal vasculature and the neuroretina are growing and differentiating in a simultaneous and coordinated fashion during the postnatal period examined, and there is a clear interdependence between them.[47,48] Therefore, disrupting the vasculature of a developing tissue such as the postnatal retina is likely to have a profound impact on its assembly and architecture. In contrast, the cornea is a fully developed avascular tissue and therefore, less likely to be affected by a compromised vasculature. It must also be noted that treatment with the anti-VEGF aptamer alone did not affect the developing retinal vessels but prevented growth of the vessels in the cornea. Because the anti-VEGF aptamer targets only a subset of all VEGF isoforms, sufficient VEGF would be available to sustain normal vessel formation. The pathological vessels of the cornea, however, may rely mostly on the pathological isoform of VEGF, $VEGF_{164}$, which is targeted by the anti-VEGF aptamer.[29]

Although PDGF-B signaling inhibition resulted in pericyte depletion of retinal and corneal vessels, it had no effect on the pericyte coverage of the adult limbal vasculature (Figure 5C), suggesting that both the susceptibility of ECs to VEGF-A withdrawal and of MCs to inhibition of PDGF-B signaling alters over time. The window of sensitivity to PDGF-B signaling inhibition is distinct though overlapping, with the window of VEGF dependency. For example, 10-day-old neovessels of the cornea, which are refractory to VEGF-A inhibition (ie, do not regress, Figure 8B), are still sensitive to PDGF-B signaling blockade. This sensitivity is reflected by the loss of pericytes and the subsequent resensitization to anti-VEGF treatment following administration of PDGF-B signaling inhibitors.

Blood vessel maturation can be characterized by a decreased sensitivity to anti-VEGF-A therapy. We speculate that there is a stage in the maturation process before the formation of a stable vessel, in which vessel endothelium are refractory to VEGF blockade but vessel pericytes are still in an immature state and susceptible to PDGF-B withdrawal. We have shown experimentally that

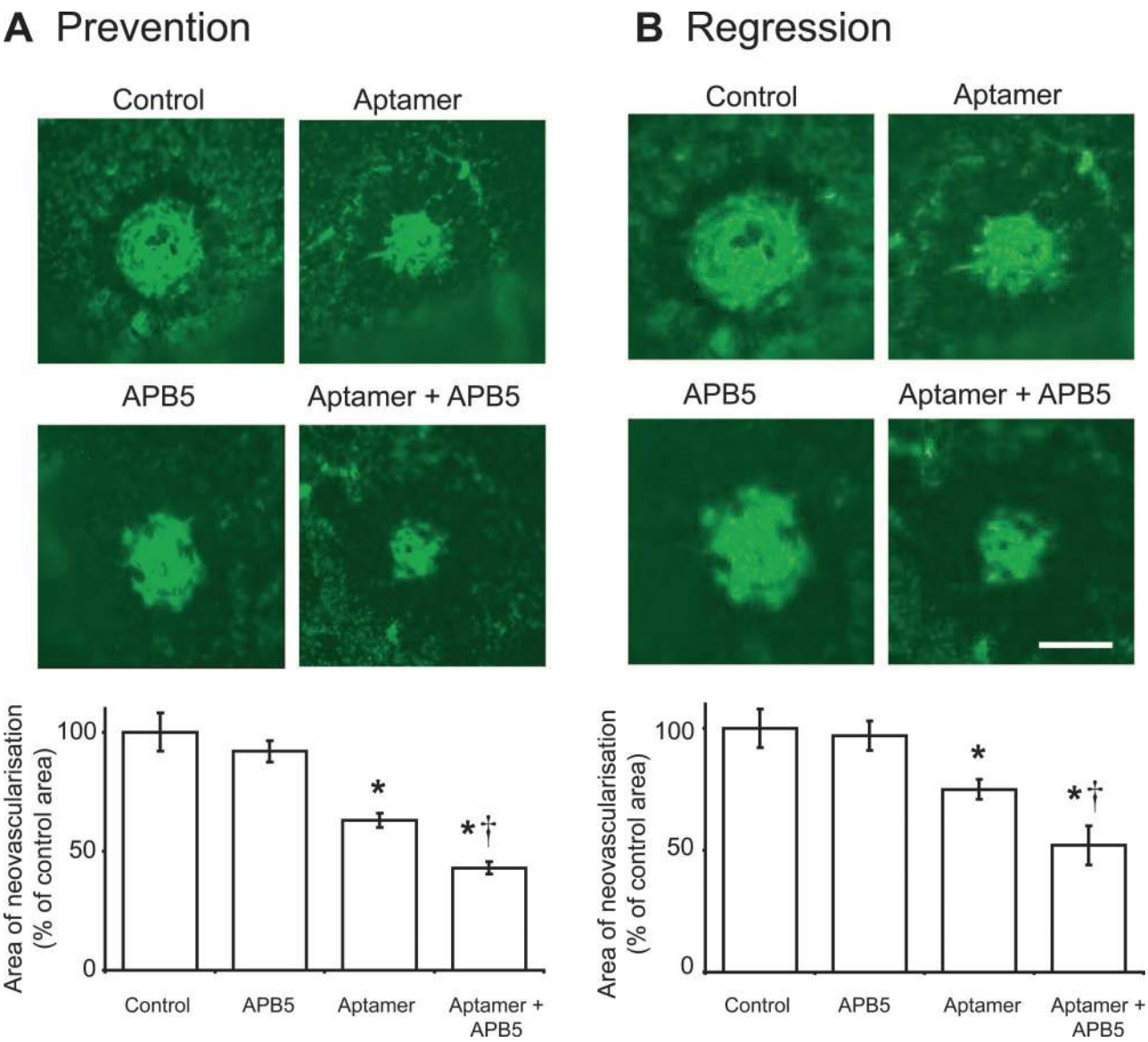

Figure 10. Combination therapy is effective both in prevention and intervention treatments of mouse CNV. **A:** Prevention: animals were treated with either APB5 or anti-VEGF aptamer or both for 14 days following laser-injury. Representative images of CNV are visualized by PECAM-1 staining. Quantitative analysis of the CNV area. $^{*}P < 0.01$ compared to control or APB5-treated mice; $^{\dagger}P < 0.05$ compared to anti-VEGF aptamer-treated mice. Combination therapy is also effective in treating later stage CNV. **B:** Mice were treated with APB5 from 7 days postinjury. At D14 postinjury, NV was analyzed after labeling vessels with PECAM-1. Quantitative analysis of CNV area. $^{*}P < 0.01$ compared to control or PDGF-B inhibitor-treated mice; $^{\dagger}P < 0.05$ compared to anti-VEGF aptamer-treated mice.

this window of PDGF-B dependency provides an opportunity to resensitize the endothelium to VEGF withdrawal, thus promoting vessel regression following combination therapy. In summary, our data suggests that, although pathological neovessels may develop resistance to anti-VEGF therapy, they can become susceptible following the inhibition of PDGF-B signaling and the ensuing MC depletion. Consequently, a combination therapy approach, using both VEGF-A and PDGF-B inhibitors, may be a more effective intervention for advanced ocular neovascular disease.

Acknowledgments

We gratefully acknowledge the excellent technical assistance with animal care, quantitative real-time PCR analysis, and electron microscopy provided by the core support services at Eyetech Research Center. We thank in particular Dr. Steve Samuelsson and Dr. William Schubert for assistance with EM quantification and Drs. Y.-S. Ng and Tracy Mitchell for comments on the manuscript.

References

1. Folkman J: Angiogenesis in cancer, vascular, rheumatoid and other disease. Nat Med 1995, 1:27–31
2. Campochiaro PA: Retinal and choroidal neovascularization. J Cell Physiol 2000, 184:301–310
3. Ferris FL, 3rd, Fine SL, Hyman L: Age-related macular degeneration and blindness due to neovascular maculopathy. Arch Ophthalmol 1984, 102:1640–1642

4. Battegay EJ: Angiogenesis: mechanistic insights, neovascular diseases, and therapeutic prospects. J Mol Med 1995, 73:333–346
5. Kwak N, Okamoto N, Wood JM, Campochiaro PA: VEGF is major stimulator in model of choroidal neovascularization. Invest Ophthalmol Vis Sci 2000, 41:3158–3164
6. Pierce EA, Avery RL, Foley ED, Aiello LP, Smith LE: Vascular endothelial growth factor/vascular permeability factor expression in a mouse model of retinal neovascularization. Proc Natl Acad Sci USA 1995, 92:905–909
7. Adamis AP, Shima DT, Tolentino MJ, Gragoudas ES, Ferrara N, Folkman J, D'Amore PA, Miller JW: Inhibition of vascular endothelial growth factor prevents retinal ischemia-associated iris neovascularization in a nonhuman primate. Arch Ophthalmol 1996, 114:66–71
8. Amano S, Rohan R, Kuroki M, Tolentino M, Adamis AP: Requirement for vascular endothelial growth factor in wound- and inflammation-related corneal neovascularization. Invest Ophthalmol Vis Sci 1998, 39:18–22
9. Robinson GS, Pierce EA, Rook SL, Foley E, Webb R, Smith LE: Oligodeoxynucleotides inhibit retinal neovascularization in a murine model of proliferative retinopathy. Proc Natl Acad Sci USA 1996, 93:4851–4856
10. Krzystolik MG, Afshari MA, Adamis AP, Gaudreault J, Gragoudas ES, Michaud NA, Li W, Connolly E, O'Neill CA, Miller JW: Prevention of experimental choroidal neovascularization with intravitreal anti-vascular endothelial growth factor antibody fragment. Arch Ophthalmol 2002, 120:338–346
11. Benjamin LE, Hemo I, Keshet E: A plasticity window for blood vessel remodelling is defined by pericyte coverage of the preformed endothelial network and is regulated by PDGF-B and VEGF. Development 1998, 125:1591–1598
12. Benjamin LE, Golijanin D, Itin A, Pode D, Keshet E: Selective ablation of immature blood vessels in established human tumors follows vascular endothelial growth factor withdrawal. J Clin Invest 1999, 103:159–165
13. Gee MS, Procopio WN, Makonnen S, Feldman MD, Yeilding NM, Lee WM: Tumor vessel development and maturation impose limits on the effectiveness of anti-vascular therapy. Am J Pathol 2003, 162:183–193
14. Sims DE: The pericyte–a review. Tissue Cell 1986, 18:153–174
15. Lindahl P, Johansson BR, Leveen P, Betsholtz C: Pericyte loss and microaneurysm formation in PDGF-B-deficient mice. Science 1997, 277:242–245
16. Hellstrom M, Kalen M, Lindahl P, Abramsson A, Betsholtz C: Role of PDGF-B and PDGFR-beta in recruitment of vascular smooth muscle cells and pericytes during embryonic blood vessel formation in the mouse. Development 1999, 126:3047–3055
17. Hellstrom M, Gerhardt H, Kalen M, Li X, Eriksson U, Wolburg H, Betsholtz C: Lack of pericytes leads to endothelial hyperplasia and abnormal vascular morphogenesis. J Cell Biol 2001, 153:543–553
18. Uemura A, Ogawa M, Hirashima M, Fujiwara T, Koyama S, Takagi H, Honda Y, Wiegand SJ, Yancopoulos GD, Nishikawa S: Recombinant angiopoietin-1 restores higher-order architecture of growing blood vessels in mice in the absence of mural cells. J Clin Invest 2002, 110:1619–1628
19. Darland DC, Massingham LJ, Smith SR, Piek E, Saint-Geniez M, D'Amore PA: Pericyte production of cell-associated VEGF is differentiation-dependent and is associated with endothelial survival. Dev Biol 2003, 264:275–288
20. Fukumura D, Xavier R, Sugiura T, Chen Y, Park EC, Lu N, Selig M, Nielsen G, Taksir T, Jain RK, Seed B: Tumor induction of VEGF promoter activity in stromal cells. Cell 1998, 94:715–725
21. Brown EB, Campbell RB, Tsuzuki Y, Xu L, Carmeliet P, Fukumura D, Jain RK: In vivo measurement of gene expression, angiogenesis and physiological function in tumors using multiphoton laser scanning microscopy. Nat Med 2001, 7:864–868
22. Bergers G, Song S, Meyer-Morse N, Bergsland E, Hanahan D: Benefits of targeting both pericytes and endothelial cells in the tumor vasculature with kinase inhibitors. J Clin Invest 2003, 111:1287–1295
23. Erber R, Thurnher A, Katsen AD, Groth G, Kerger H, Hammes HP, Menger MD, Ullrich A, Vajkoczy P: Combined inhibition of VEGF and PDGF signaling enforces tumor vessel regression by interfering with pericyte-mediated endothelial cell survival mechanisms. FASEB J 2004, 18:338–340
24. Pietras K, Ostman A, Sjoquist M, Buchdunger E, Reed RK, Heldin CH, Rubin K: Inhibition of platelet-derived growth factor receptors reduces interstitial hypertension and increases transcapillary transport in tumors. Cancer Res 2001, 61:2929–2934
25. Pietras K, Rubin K, Sjoblom T, Buchdunger E, Sjoquist M, Heldin CH, Ostman A: Inhibition of PDGF receptor signaling in tumor stroma enhances antitumor effect of chemotherapy. Cancer Res 2002, 62:5476–5484
26. Klein R, Wang Q, Klein BE, Moss SE, Meuer SM: The relationship of age-related maculopathy, cataract, and glaucoma to visual acuity. Invest Ophthalmol Vis Sci 1995, 36:182–191
27. Ruckman J, Green LS, Beeson J, Waugh S, Gillette WL, Henninger DD, Claesson-Welsh L, Janjic N: 2′-Fluoropyrimidine RNA-based aptamers to the 165-amino acid form of vascular endothelial growth factor (VEGF165). Inhibition of receptor binding and VEGF-induced vascular permeability through interactions requiring the exon 7-encoded domain. J Biol Chem 1998, 273:20556–20567
28. Eyetech Study Group: Preclinical and phase 1A clinical evaluation of an anti-VEGF pegylated aptamer (EYE001) for the treatment of exudative age-related macular degeneration. Retina 2002, 22:143–152
29. Ishida S, Usui T, Yamashiro K, Kaji Y, Amano S, Ogura Y, Hida T, Oguchi Y, Ambati J, Miller JW, Gragoudas ES, Ng YS, D'Amore PA, Shima DT, Adamis AP: VEGF164-mediated inflammation is required for pathological, but not physiological, ischemia-induced retinal neovascularization. J Exp Med 2003, 198:483–489
30. Joussen AM, Poulaki V, Mitsiades N, Stechschulte SU, Kirchhof B, Dartt DA, Fong GH, Rudge J, Wiegand SJ, Yancopoulos GD, Adamis AP: VEGF-dependent conjunctivalization of the corneal surface. Invest Ophthalmol Vis Sci 2003, 44:117–123
31. Mori K, Ando A, Gehlbach P, Nesbitt D, Takahashi K, Goldsteen D, Penn M, Chen CT, Melia M, Phipps S, Moffat D, Brazzell K, Liau G, Dixon KH, Campochiaro PA: Inhibition of choroidal neovascularization by intravenous injection of adenoviral vectors expressing secretable endostatin. Am J Pathol 2001, 159:313–320
32. Livak KJ, Schmittgen TD: Analysis of relative gene expression data using real-time quantitative PCR and the 2(-Delta Delta C(T)) Method. Methods 2001, 25:402–408
33. Morikawa S, Baluk P, Kaidoh T, Haskell A, Jain RK, McDonald DM: Abnormalities in pericytes on blood vessels and endothelial sprouts in tumors. Am J Pathol 2002, 160:985–1000
34. Ruhrberg C, Gerhardt H, Golding M, Watson R, Ioannidou S, Fujisawa H, Betsholtz C, Shima DT: Spatially restricted patterning cues provided by heparin-binding VEGF-A control blood vessel branching morphogenesis. Genes Dev 2002, 16:2684–2698
35. Zondor SD, Medina PJ: Bevacizumab: an angiogenesis inhibitor with efficacy in colorectal and other malignancies. Ann Pharmacother 2004, 38:1258–1264
36. Gragoudas ES, Adamis AP, Cunningham ET, Jr., Feinsod M, Guyer DR: Pegaptanib for neovascular age-related macular degeneration. N Engl J Med 2004, 351:2805–2816
37. Adamis AP, Shima DT: The role of vascular endothelial growth factor in ocular health and disease. Retina 2005, 25:111–118
38. Tobe T, Ortega S, Luna JD, Ozaki H, Okamoto N, Derevjanik NL, Vinores SA, Basilico C, Campochiaro PA: Targeted disruption of the FGF2 gene does not prevent choroidal neovascularization in a murine model. Am J Pathol 1998, 153:1641–1646
39. Moromizato Y, Stechschulte S, Miyamoto K, Murata T, Tsujikawa A, Joussen AM, Adamis AP: CD18 and ICAM-1-dependent corneal neovascularization and inflammation after limbal injury. Am J Pathol 2000, 157:1277–1281
40. Darland DC, D'Amore PA: Blood vessel maturation: vascular development comes of age. J Clin Invest 1999, 103:157–158
41. Ferrara N: Vascular endothelial growth factor: basic science and clinical progress. Endocr Rev 2004, 25:581–611
42. Lindheimer MD: Unraveling the mysteries of preeclampsia. Am J Obstet Gynecol 2005, 193:3–4
43. Sundberg C, Kowanetz M, Brown LF, Detmar M, Dvorak HF: Stable expression of angiopoietin-1 and other markers by cultured pericytes: phenotypic similarities to a subpopulation of cells in maturing vessels

during later stages of angiogenesis in vivo. Lab Invest 2002, 82:387–401
44. Abramsson A, Berlin O, Papayan H, Paulin D, Shani M, Betsholtz C: Analysis of mural cell recruitment to tumor vessels. Circulation 2002, 105:112–117
45. Chekenya M, Enger PO, Thorsen F, Tysnes BB, Al-Sarraj S, Read TA, Furmanek T, Mahesparan R, Levine JM, Butt AM, Pilkington GJ, Bjerkvig R: The glial precursor proteoglycan, NG2, is expressed on tumour neovasculature by vascular pericytes in human malignant brain tumours. Neuropathol Appl Neurobiol 2002, 28:367–380
46. Falcon BL, Sennino B, Grate D, Epstein DM, McDonald DM: Aptamers Specifically Targeting PDGF-B Decrease Blood Vessels and Pericytes in Tumors. Presented at the FASEB Experimental Biology, San Diego, CA, 2005
47. Zhang Y, Porat RM, Alon T, Keshet E, Stone J: Tissue oxygen levels control astrocyte movement and differentiation in developing retina. Brain Res Dev Brain Res 1999, 118:135–145
48. West H, Richardson WD, Fruttiger M: Stabilization of the retinal vascular network by reciprocal feedback between blood vessels and astrocytes. Development 2005, 132:1855–1862